PHYSICAL REVIEW C **88**, 021301(R) (2013)

# Unexpected characteristics of the isoscalar monopole resonance in the $A \approx 90$ region: Implications for nuclear incompressibility

D. H. Youngblood,[1] Y.-W. Lui,[1] Krishichayan,[1,2] J. Button,[1] M. R. Anders,[1] M. L. Gorelik,[3] M. H. Urin,[3] and S. Shlomo[1]
[1]*Cyclotron Institute, Texas A&M University, College Station, Texas 77843, USA*
[2]*Department of Pure and Applied Physics, Guru Ghasidas University, Bilaspur, 495009, Chhattisgarh, India*
[3]*National Research Nuclear University "MEPhI," Moscow 115409, Russia*
(Received 8 March 2013; published 14 August 2013)

The isoscalar giant monopole resonances (ISGMRs) in $^{90,92,94}$Zr and $^{92,96,98,100}$Mo have been studied with inelastic scattering of 240-MeV $\alpha$ particles at small angles including 0°. Strength corresponding to approximately 100% of the ISGMR ($E0$) energy-weighted sum rule was identified in each nucleus. In all cases the strength consisted of two components separated by 7–9 MeV. Except for the mass 92 nuclei, the upper component contained 14–22% of the $E0$ energy-weighted sum rule (EWSR); however 38% and 65% of the $E0$ EWSR were located in the upper components in $^{92}$Zr and $^{92}$Mo, respectively. The energies of the ISGMRs for $^{92}$Zr and $^{92}$Mo are 1.22 and 2.80 MeV, respectively, higher than for $^{90}$Zr, suggesting a significant nuclear structure contribution to the energy of the ISGMR in these nuclei. This has a large effect on the compression modulus of the nucleus with the values extracted for $^{92}$Zr and $^{92}$Mo being 27 and 56 MeV, respectively, higher than that for $^{90}$Zr.

DOI: 10.1103/PhysRevC.88.021301 PACS number(s): 24.30.Cz, 25.55.Ci, 27.60.+j

The isoscalar giant monopole resonance (ISGMR) is of particular interest because its energy $E_{\rm GMR}$ can be directly related to the compression modulus of the nucleus ($K_A$) [1,2] as follows:

$$E_{\rm GMR}=(\hbar^2 K_A/m\langle r^2\rangle)^{1/2}, \qquad (1)$$

where $m$ is the nucleon mass and $\langle r^2\rangle$ is the mean square nuclear radius. Using the $A^{1/3}$ expansion of $K_A$, the compressibility of nuclear matter, $K_{\rm NM}$, which is important in understanding the behavior of stars and heavy ion reactions, can be obtained [1,2]. However it is common to determine $K_{\rm NM}$ by carrying out microscopic calculations of $E_{\rm GMR}$ within the Hartree-Fock (HF)-based random-phase approximation (RPA) using effective nucleon-nucleon interactions [1,3–5] and comparing the results with the experimental values of $E_{\rm GMR}$, exploiting the sensitivity of the calculated $E_{\rm GMR}$ to the value of $K_{\rm NM}$ associated with the effective interaction. In 1999, measurements of the ISGMRs for $^{40}$Ca, $^{90}$Zr, $^{116}$Sn, $^{144}$Sm, and $^{208}$Pb [6] were compared to HF-based RPA calculations which used the Gogny interaction [3] and took into account pairing and anharmonicity corrections, and a value of $K_{\rm NM} = 231 \pm 5$ MeV was obtained. These data were of considerably higher quality than data from the 1970s and 1980s (for a summary of these data see Ref. [7]) which had been previously used to extract nuclear compressibility.

In this paper we report on measurements of the ISGMRs in $^{90,92,94}$Zr and $^{92,96,98,100}$Mo where the GMR energies in the $A = 92$ nuclei yield nuclear compressibilities substantially higher than those of the other nuclei in this region (~27 MeV higher for $^{92}$Zr and ~56 MeV higher for $^{92}$Mo). These differences are not predicted with HF-based RPA calculations that reproduce the ISGMR energies in the other isotopes and that are generally used to relate $K_{\rm NM}$ to $K_A$. The origin of this discrepancy is unknown and raises the question of what is left out of such calculations and how do these omissions affect $K_{\rm NM}$.

The measurements were made with inelastic scattering of 240-MeV $\alpha$ particles at small angles including 0°. The experimental technique has been described previously [8] and is summarized below. Beams of 240-MeV $\alpha$ particles from the Texas A&M K500 superconducting cyclotron bombarded self-supporting Zr and Mo foils 5–8 mg/cm$^2$ thick, each enriched to more than 96% in the desired isotope, located in the target chamber of the multipole-dipole-multipole spectrometer. The horizontal and vertical acceptance of the spectrometer was 4° and ray tracing was used to reconstruct the scattering angle. The focal plane detector measured position and angle in the scattering plane and covered from $E_x \sim 8$ MeV to $E_x > 55$ MeV. Cross sections were obtained from the charge collected, target thickness, dead time, and known solid angle. Target thicknesses were measured by weighing and checked by measuring the energy loss of the 240-MeV $\alpha$ beam in each target. The cumulative uncertainties in target thickness, solid angle, etc., result in about a ±10% uncertainty in absolute cross sections.

Initially data were taken for $^{90,92}$Zr and $^{92,96,100}$Mo and analysis revealed the behavior in the $A = 92$ nuclei reported here. In an additional experimental run, data were taken for $^{92}$Mo, $^{94}$Zr, and $^{98}$Mo. The $^{92}$Mo strength distributions obtained in the two experiments are in excellent agreement.

Sample spectra obtained are shown in Fig. 1. The spectrum was divided into a peak and a continuum where the continuum was assumed to have the shape of a straight line at high excitation joining onto a Fermi shape at low excitation to model particle threshold effects [9]. Samples of the continua used are shown in Fig. 1. The giant resonance peak can be seen extending up to $E_x \sim 35$ MeV.

Single-folding density-dependent distorted-wave Born approximation calculations (described in Ref. [10]) were carried out with Fermi mass distributions and collective transition densities using optical potentials obtained for $^{90}$Zr [9]. The multipole components of the giant resonance peak were obtained as described in Ref. [9] and the (isoscalar) $E0$ multipole distributions obtained are shown in Fig. 2. Several analyses were carried out to assess the effects of different

 

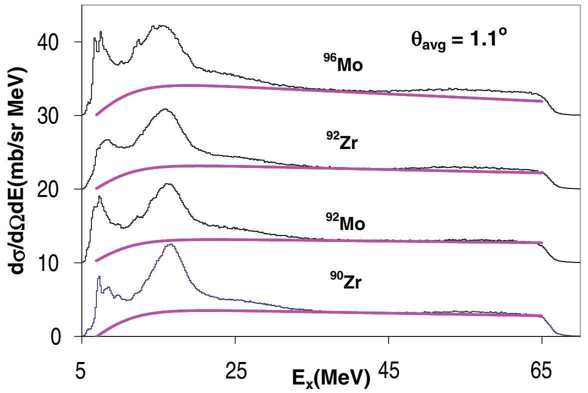


FIG. 1. (Color online) Inelastic $\alpha$ spectra obtained with the spectrometer at 0° for $^{90}$Zr, $^{92}$Mo (offset 10 units), $^{92}$Zr (offset 20 units), and $^{96}$Mo (offset 30 units). The thick lines show continua chosen for the analysis.

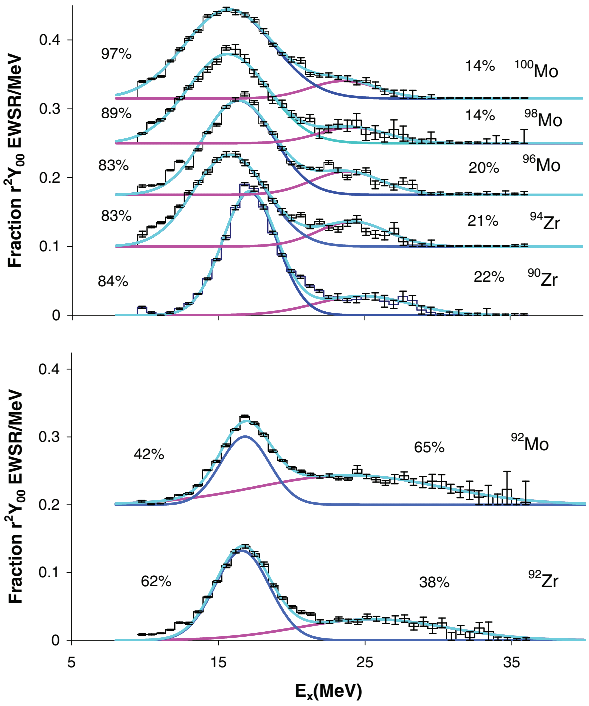


FIG. 2. (Color online) The black histograms show the fraction of the $r^2Y_{00}$ sum rule obtained for Mo and Zr isotopes plotted as a function of excitation energy. Superimposed are Gaussian fits to the two components of the distributions as well as the sum of the fits. On the left side are the strengths of the lower energy peak while on the right side the strengths of the higher energy peaks are listed, all given as a percentage of the $r^2Y_{00}$ sum rule.

choices of the continuum on the multipole distributions as described in Ref. [9]. The errors shown on the strength distributions were calculated by adding the errors obtained from the multipole fits in quadrature to the standard deviations between the different analyses. Energies and sum rule strengths obtained are summarized in Table I. The $E0$ strength identified in each nucleus corresponded within errors to 100% of the $E0$ energy-weighted sum rule (EWSR). The results obtained for $^{90}$Zr are in excellent agreement with our previous results [6,9]. While $E_{\rm GMR}$ generally decreases as $A$ increases (this is small in adjacent nuclei), $E_{\rm GMR}$ for $^{92}$Zr and $^{92}$Mo are 1.22 and 2.80 MeV, respectively, higher than for $^{90}$Zr, a surprising result.

In all of these nuclei, the $E0$ strength consists of a relatively narrow peak, with significant tailing at higher excitation. To provide a consistent framework to compare the results for the different nuclei, the $E0$ distributions were fit with two Gaussians. For the nuclei with $A \neq 92$, 80–90% of the strength is in the lower energy peak located at 15.7 to 17.2 MeV, with the remaining 10 to 20% located in a broad peak centered at $E_x \sim 25$ MeV. It is clear that the distribution of the $E0$ strength in $^{92}$Mo is dramatically different from the others, with only 40% of the observed strength in the lower peak and 60% in the upper peak. In $^{92}$Zr, the lower peak contains 65% and the upper peak 35% of the observed $E0$ strength. While the overall $E0$ strength could be affected somewhat by raising or lowering the assumed continuum, the dramatic difference in strength distributions between $^{90}$Zr and $^{92}$Mo could be reduced significantly only by assuming that the shape and strength of the continuum changes radically relative to the strength above the resonance region as a function of angle and changes very differently for different nuclei. The isoscalar giant quadrupole resonance (GQR) is located just below the ISGMR and the GQR strength extracted for all the nuclei is concentrated in

TABLE I. Parameters obtained for the $E0$ distributions shown in Fig. 2. Uncertainties include systematic errors. $E_{\rm GMR}$ is given by the ratio of energy moments $(m_3/m_1)^{1/2}$ for the scaling model [2].

| Nucleus | %$E0$ EWSR | $E_{\rm GMR}$ $(m_3/m_1)^{1/2}$ (MeV) | Centroid $m_1/m_0$ (MeV) | Gaussian fit: Low peak $E_x$ (MeV) | Low peak $\Gamma$ (MeV) | %$E0$ EWSR | High peak $E_x$ (MeV) | High peak $\Gamma$ (MeV) | %E0 EWSR |
|---|---|---|---|---|---|---|---|---|---|
| $^{90}$Zr | 106 ± 12 | 18.86 + 0.23–0.14 | 17.88 + 0.13–0.11 | 17.1 | 4.4 | 84 | 24.9 | 7.6 | 22 |
| $^{92}$Zr | 103 ± 12 | 20.09 + 0.31–0.22 | 18.23 + 0.15–0.13 | 16.6 | 4.4 | 62 | 25.5 | 12.0 | 38 |
| $^{94}$Zr | 106 ± 12 | 17.52 + 0.18–0.14 | 16.16 + 0.12–0.11 | 15.8 | 5.9 | 83 | 24.2 | 5.6 | 21 |
| $^{92}$Mo | 107 ± 13 | 21.68 + 0.53–0.33 | 19.62 + 0.28–0.19 | 16.8 | 4 | 42 | 23.9 | 14.7 | 65 |
| $^{96}$Mo | 105 ± 12 | 18.18 + 0.20–0.13 | 16.95 + 0.12–0.10 | 16.4 | 5.7 | 83 | 23.8 | 5.7 | 20 |
| $^{98}$Mo | 103 ± 12 | 17.29 + 0.46–0.21 | 16.01 + 0.19–0.13 | 15.7 | 6.5 | 89 | 24.2 | 5.6 | 14 |
| $^{100}$Mo | 110 ± 12 | 17.35 + 0.16–0.12 | 16.13 + 0.11–0.10 | 15.8 | 7.1 | 97 | 23.6 | 5.5 | 14 |

symmetrical peaks containing 80 ∼ 95% of the $E2$ EWSR. In $^{90}$Zr, $^{92}$Zr, and $^{92}$Mo, $E_{\rm GQR} = 14.30 \pm 0.15, 14.02 \pm 0.15$, and $14.53 \pm 0.15$ MeV, respectively, having rms widths of 4.8, 5.5, and 6.3 MeV. There is no tailing of the quadrupole strength in any of the nuclei studied and $E_{\rm GQR}$ for the mass 92 nuclei are within errors the same as $^{90}$Zr.

Prior to our 240-MeV $\alpha$ work reported in 1999 [6], the strength in $^{90}$Zr at ∼23–25 MeV had not been seen due in part to the much higher continuum/background present in the earlier (lower energy) studies [11,12] and in part to the assumption that any strength above the unresolved GQR-ISGMR peak was part of the continuum/background. In these earlier works it was also assumed that the strength in each giant resonance was concentrated in a single Gaussian peak.

A study of $^{90}$Zr at Osaka with 400-MeV $\alpha$ particles [13] showed the $E0$ strength with a peak at $E_x = 16.6$ MeV and continuous $E0$ strength through 32 MeV, the highest energy reported, which would mask the strength we see. Most of the multipole distributions in most of the nuclei reported by the Osaka group [13,14] show continuous strength above the giant resonance peak to the highest energy studied, and they argue that this continuous strength must be spurious. In most cases, if this strength were real, they would identify significantly more than 100% of the EWSR for each multipole.

The ISGMRs in $^{92}$Mo and $^{96}$Mo were studied with $^3$He inelastic scattering [11] in 1983; 24 and 19% of the $E0$ EWSR, respectively, were located in Gaussian peaks at $E_x = 16.35$ and 16.40 MeV, respectively. The same group later used 152-MeV $\alpha$ inelastic scattering [15] to study $^{92}$Mo and reported $84 \pm 17\%$ of the strength in a peak at $E_x = 16.2$ MeV with a width $\Gamma = 4.8$ MeV. Though both $^3$He and $\alpha$ results are listed in the table in Ref. [15], the authors do not comment on the reason for the discrepancy between them. In both these works, the authors assumed that the $E0$ strength was located in a single Gaussian peak and all cross sections at energies above $E_x \sim 21$ MeV were attributed to the continuum/background. We now know that giant resonance strength extends up to $E_x \sim 35$ MeV in most nuclei [6,8,9,16]. Their continuum/background assumptions precluded identification of any strength above $E_x \sim 21$ MeV. The calculations used to normalize the strength were carried out with the deformed potential model, and it has been shown [17] that reliable strengths can be obtained only with folding calculations, so that the uncertainties would be larger if the uncertainties in the calculations were included.

Within the scaling model [2], the ISGMR energy is given by $E_{\rm GMR} = (m_3/m_1)^{1/2}$, where $m_k$ is the $k$th energy moment of the strength distribution. Using for $E_{\rm GMR}$ the experimental energies corresponding to the scaling model $\{(m_3/m_1)^{1/2}\}$ shown in Table I and radii obtained from Hartree-Fock calculations [18] with the KDE0v1 interaction [4] having $K_{\rm NM} = 227.5$ MeV, the experimental scaling model values of $K_A$ for the Zr and Mo isotopes were obtained from Eq. (1) and are plotted versus $A$ in Fig. 3. For $^{92}$Zr and $^{92}$Mo, $K_A$ values obtained from the experimental energies are 27 MeV ($5\sigma$) and 56 MeV ($8\sigma$) higher than the values predicted with HF-based RPA.

In an attempt to understand why so much of the $E0$ strength lies at higher excitation in $^{92}$Mo, microscopic energy-

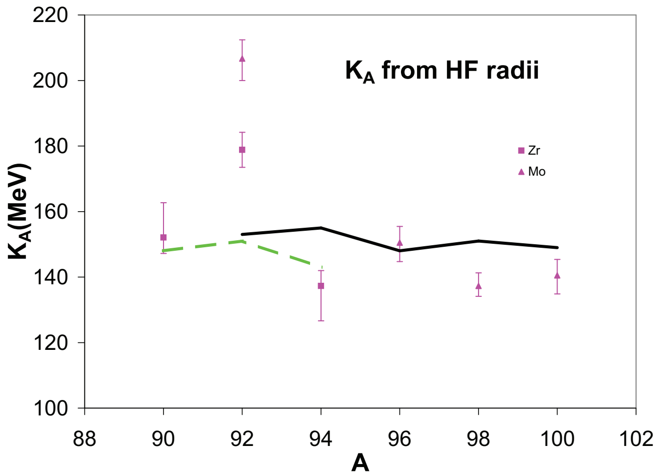


FIG. 3. (Color online) The scaling model $K_A$ values obtained from the measured scaling energies $(m_3/m_1)^{1/2}$ are shown for the Zr isotopes by squares and for the Mo isotopes by the triangles plotted versus $A$. The error bars reflect the uncertainties in $(m_3/m_1)^{1/2}$. Also shown are lines connecting the HF-based RPA values of $K_A$ calculated within HF-RPA using the KDE0v1 interaction for the Zr (green dashed line) and Mo (black line) isotopes.

dependent transition densities were calculated for $^{92}$Mo within continuum RPA [19] and used to calculate cross sections for $E0$ excitation at $E_x = 17.5$ and 27.5 MeV, roughly representing excitation into the two components of the $E0$ strength. Using the collective transition density, the cross section predicted for excitation of the ISGMR at $E_x = 27.5$ MeV was ∼1/5 that at $E_x = 17.5$ MeV, whereas with the energy-dependent microscopic transition densities this ratio was ∼1/12. The $E0$ strength is plotted as a fraction of the $E0$ EWSR which is obtained by dividing the experimental value by the predicted value. Thus the decrease in the predicted value obtained using the microscopic transition density will *increase* the upper peak by more than a factor of 2 in $^{92}$Mo, resulting in the upper peak alone exhausting more than 100% of the EWSR and shifting $E_{\rm GMR}$ to even higher energy, further increasing $K_A$ for $^{92}$Mo.

We also investigated the possibility that this second peak could be the "overtone" ISGMR using the corresponding scattering operator $f(r)Y_{00}$ [20], where

$$f(r) = r^4 - 2r^2\langle r^4\rangle/\langle r^2\rangle.$$

Using the collective transition density and sum rule for the overtone, two calculations were done for $^{92}$Mo. The first assumed that the second peak was entirely due to the overtone. That would require 228% of the $f(r)Y_{00}$ sum rule for the overtone and leave only 42% of the $r^2Y_{00}$ sum rule in the lower peak [Fig. 4(a)]. We then calculated the strength assuming the overtone was at twice the energy of the narrow peak with twice the width, with 100% of the $f(r)Y_{00}$ sum rule, and subtracted that from the $^{92}$Mo $E0$ strength shown in Fig. 2. This is shown in Fig. 4(b). This leaves the $E0$ strength corresponding to 91% of the $r^2Y_{00}$ sum rule, which is quite plausible. The error bar shown represents the uncertainty in the $E0$ strength extracted from the data and is sufficiently large that the negative

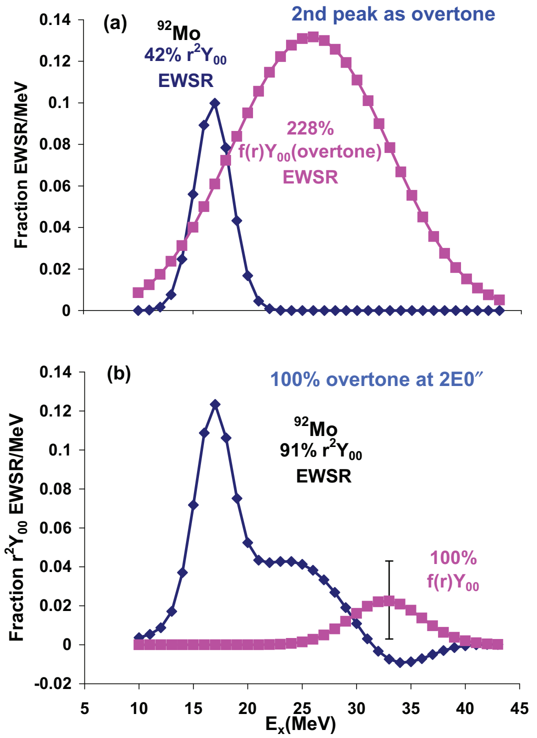


FIG. 4. (Color online) (a) ISGMR strength distributions for $^{92}$Mo obtained by assuming that the lower peak (diamonds) is due entirely to ISGMR excitation and the upper peak (squares) is due entirely to overtone excitation are plotted versus excitation energy. The percentages of the respective sum rules are indicated. The vertical scale for the lower peak is relative to the $r^2Y_{00}$ sum rule, while that for the upper peak is relative to the $f(r)Y_{00}$ sum rule. (b) The strength distribution obtained for the overtone in $^{92}$Mo located at twice the energy of the lower peak with twice the width and containing 100% of the $f(r)Y_{00}$ sum rule is shown by the squares plotted versus excitation energy. The diamonds show the strength remaining after this is subtracted from the strength shown in Fig. 2. The vertical scale is relative to the $r^2Y_{00}$ sum rule. The error bar indicates the experimental error at $E_x = 33$ MeV.

strength remaining after the subtraction is smaller than the experimental error. $E_{\rm GMR}$ for the calculation in the bottom panel is 20.15 MeV, resulting in $K_A$ of 179 MeV, 27 MeV above that expected from the HF-based RPA calculations. While this reduces the discrepancy for $^{92}$Mo (and could eliminate it for $^{92}$Zr), there is no obvious reason for the overtone to be present in $A = 92$ nuclei and absent for the other nuclei.

Thus we are left with the conclusion that the $E0$ strength distributions observed are due to the ISGMR and those in the $A = 92$ nuclei lead to nuclear compressibilities (particularly for $^{92}$Mo) much higher than those of the other nuclei in this region, which raises serious questions about the influence of the nuclear structure on the energy of the ISGMR and thus about nuclear matter compressibility extracted from these energies. The ISGMR energy is significantly affected by the properties of the individual nucleus in a manner not accounted for in HF-based RPA calculations that relate ISGMR energies to $K_{\rm NM}$ and thus is not a good indicator of compressibility in these $A = 92$ nuclei.

There are at least two other cases where measured ISGMR energies seem to lead to anomalous results for $K_{\rm NM,}$ though not nearly as large as for $^{92}$Mo. The ISGMR strength in the Sn isotopes has been measured at both TAMU [8,21] and Osaka [14] and while there are significant disagreements between them, both show the ISGMR in the Sn isotopes at lower energy than expected, which would require a compressibility lower than that obtained from the ISGMR energies in many other nuclei [22,23].

Recently, Lui *et al.* [16] showed that the ISGMR in $^{48}$Ca is at higher energy than in $^{40}$Ca, a feature not reproduced in HF-based RPA calculations. While it might be expected that nuclear structure would play a bigger role in light nuclei, in Ref. [6] it was shown that the ISGMR location in $^{40}$Ca was consistent with $K_{\rm NM}$ obtained from heavier nuclei.

The basic assumption used to obtain the incompressibility of nuclear matter from the energy of the ISGMR has been that this energy is not affected by the details of the nuclear structure beyond the general features contained in the calculation of the ISGMR location for a particular nucleus. The results reported here for $^{92}$Zr and $^{92}$Mo obviously challenge that assumption.

This work was supported in part by the US Department of Energy under Grant No. DE-FG03-93ER40773.

[1] J. P. Blaizot, Phys. Rep. **64**, 171 (1980).
[2] J. Treiner, H. Krivine, and O. Bohigas, Nucl. Phys. A **371**, 253 (1981).
[3] P. Blaizot *et al.*, Nucl. Phys. A **591**, 435 (1995).
[4] B. K. Agrawal, S. Shlomo, and V. K. Au, Phys. Rev. C **72**, 014310 (2005).
[5] S. Shlomo, V. M. Kolomietz, and G. Colo, Eur. Phys. J A **30**, 23 (2006).
[6] D. H. Youngblood, H. L. Clark, and Y.-W. Lui, Phys. Rev. Lett. **82**, 691 (1999).
[7] S. Shlomo and D. H. Youngblood, Phys. Rev. C **47**, 529 (1993).
[8] D. H. Youngblood, Y.-W. Lui, H. L. Clark, B. John, Y. Tokimoto, and X. Chen, Phys. Rev. C **69**, 034315 (2004).
[9] D. H. Youngblood, Y.-W. Lui, B. John, Y. Tokimoto, H. L. Clark, and X. Chen, Phys. Rev. C **69**, 054312 (2004).
[10] Y.–W. Lui, D. H. Youngblood, Y. Tokimoto, H. L. Clark, and B. John, Phys. Rev. C **69**, 034611 (2004).
[11] M. Buenerd, in *Proceedings of International Symposium on Highly Excited States and Nuclear Structure, Orsay, France*, edited by N. Marty and N. Van Giai, J. Phys. (Paris), Colloq. **45**, C4-115 (1984).
[12] D. H. Youngblood, P. Bogucki, J. D. Bronson, U. Garg, Y.-W. Lui, and C. M. Rozsa, Phys. Rev. C **23**, 1997 (1981).
[13] M. Uchida *et al.*, Phys. Rev. C **69**, 051301(R) (2004).
[14] T. Li *et al.*, Phys. Rev. Lett. **99**, 162503 (2007); Phys. Rev. C **81**, 034309 (2010).

[15] G. Duhamel, M. Buenerd, P. de Saintignon, J. Chauvin, D. Lebrun, Ph. Martin, and G. Perrin, Phys. Rev. C **38**, 2509 (1988).
[16] Y.-W. Lui, D. H. Youngblood, S. Shlomo, X. Chen, Y. Tokimoto, Krishichayan, M. Anders, and J. Button, Phys. Rev. C **83**, 044327 (2011).
[17] J. R. Beene, D. J. Horen, and G. R. Satchler, Phys. Lett. B **344**, 67 (1995).
[18] M. R. Anders and S. Shlomo (private communication).
[19] M. L. Gorelik, I. V. Safonov, and M. H. Urin, Phys. Rev. C **69**, 054322 (2004).
[20] S. Shlomo, V. M. Kolomietz, and B. K. Agrawal, Phys. Rev. C **68**, 064301 (2003).
[21] Y.-W. Lui, D. H. Youngblood, Y. Tokimoto, H. L. Clark, and B. John, Phys. Rev. C **70**, 014307 (2004).
[22] J. Piekarewicz, Phys. Rev. C **76**, 031301(R) (2007).
[23] U. Garg *et al*., Nucl. Phys. A **788**, 36c (2007).